Materials & Design 217 (2022) 110661

Contents lists available at ScienceDirect

Materials & Design

journal homepage: www.elsevier.com/locate/matdes

Biomimetic hierarchical nanofibrous surfaces inspired by superhydrophobic lotus leaf structure for preventing tissue adhesions

Marketa Klicova [a,*], Zuzana Oulehlova [a], Andrea Klapstova [a], Matěj Hejda [b], Michal Krejcik [c], Ondrej Novak [a], Jana Mullerova [c], Jakub Erben [a], Jachym Rosendorf [d], Richard Palek [d], Vaclav Liska [d], Anna Fucikova [e], Jiri Chvojka [a], Iveta Zvercova [f], Jana Horakova [a]

[a] Department of Nonwovens and Nanofibrous Materials, Faculty of Textile Engineering, Technical University of Liberec, Studentska 2, 461 17 Liberec, Czech Republic
[b] Institute of Photonics, Dept. of Physics, University of Strathclyde, 99 George Street, Glasgow G11RD, UK
[c] The Institute for Nanomaterials, Advanced Technologies and Innovation, Technical University of Liberec, Bendlova 7, 460 01 Liberec, Czech Republic
[d] Biomedical Center, Faculty of Medicine in Pilsen, Charles University, Alej Svobody 1655/76, 323 00 Plzen, Czech Republic
[e] Charles University, Faculty of Mathematics and Physic, Department of Chemical Physic and Optics, Ke Karlovu 3, Prague 12116 2, Czech Republic
[f] Department of Science and Research, Faculty of Health Studies, Technical University of Liberec, Studentska 2, 461 17 Liberec, Czech Republic

HIGHLIGHTS

- The novel material was developed to prevent serious postoperative adhesions.
- The large-scale fabrication was optimized, aiming towards a market-ready product.
- The reduced tissue adhesion was evaluated *ex vivo* to avoid excessive animal use.
- Application is convenient for surgeons, does not require prolonged operation time.
- The material structure also holds promise for self-cleaning surfaces or membranes.

GRAPHICAL ABSTRACT

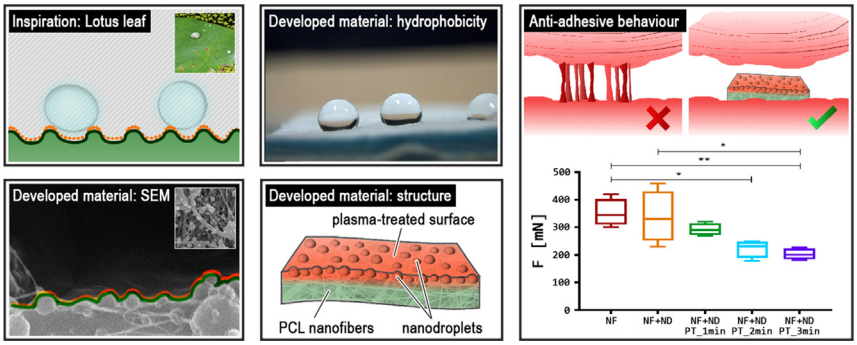

ARTICLE INFO

Article history:
Received 29 January 2022
Revised 5 April 2022
Accepted 12 April 2022
Available online 15 April 2022

Keywords:
Nanofiber membrane
Lotus effect
Antiadhesive barrier
Postoperative adhesion
Needleless electrospraying

ABSTRACT

Undesirable tissue adhesions remain one of the most common and dreaded postoperative complications. Biocompatible nanofibrous mats with antiadhesive surfaces represent a promising barrier method for preventing the formation of adhesions. The material developed in this work was inspired by the natural superhydrophobic lotus leaf nanostructure, which was mimicked by a unique combination of needleless electrospraying and electrospinning technology of poly-ε-caprolactone (PCL). The surface hydrophobicity of electrosprayed nanodroplets was further enhanced by cold plasma modification using the chemical vapor deposition (CVD) method with hexamethyldisiloxane (HMDSO). The treatment led to a successful decrease in surface wettability of our samples. Morphology (scanning electron microscopy), wettability (contact angle) and chemical composition (FTIR analysis) were observed for a period of six months to track possible changes; the obtained results verified the presence of HMDSO during the whole time period. Cytocompatibility was confirmed *in vitro* with 3T3 mouse fibroblasts according to the norm ISO 10993-5. Cell adhesion and proliferation were assessed *in vitro* by metabolic MTT assay and fluorescence microscopy after 4, 7, and 14 days. Antiadhesive behaviour was confirmed by atomic force microscopy

* Corresponding author.
E-mail address: marketa.klicova@tul.cz (M. Klicova).

https://doi.org/10.1016/j.matdes.2022.110661

and *ex vivo* by peel test 90° with intestinal tissue, the final structure has a great potential to reduce post-operative tissue adhesions.

1. Introduction

Functionalized nanofibrous materials with a complex structure are receiving constantly growing attention since nanofibrous layers alone do not meet the ever-increasing demands of medicine and tissue engineering. One of the current requirements, coming directly from physicians in clinical practice, is the creation of biocompatible antiadhesive materials. These materials serve as antiadhesive barrier agents in prevention of the dreaded postoperative adhesions, which happen after surgery in tendon, dural sac, pericardium, pelvis, or abdominal area [1]. Impacts of these complications depend on the location of the performed surgical procedure; for instance, in gastrointestinal surgery can lead to intestinal obstruction, intestinal passage disorders, infertility, reoperation, and reduced quality of life after surgery [2].

This study focuses on development of a novel biocompatible nanofibrous scaffold to meet the strict requirement of modern medicine and help to reduce tissue adhesion. In general, the material's surface properties affect biocompatibility, protein adhesion, cell growth, and proliferation. When modifying fibrous scaffolds, it is usually desirable to maintain the bulk properties and change only its surface [3]. The adhesive behaviour is mainly influenced by the chemical composition and morphology of the surface [4,5]. Another critical parameter is surface wettability. It has been shown that cells adhere better to hydrophilic materials, forming a contact angle between the material and a drop of water <90° [6]. The adsorption of proteins and cells can be controlled by altering the sample surface structure, where the roughness at the micro and nanoscale matters the most. The surface topography changes can be obtained by manufacturing or chemical surface functionalization, such as plasma treatment [4]. By increasing the surface micro-roughness and by plasma modification with hydrophobic agents, it is possible to radically change the contact angle of the material. Dowling et al. changed the typical contact angle of polystyrene (90°) to a superhydrophobic material (155°) by altering the surface roughness via grinding and chemistry by plasma treatment [7].

Several approaches have been found in the literature that have been used to prepare fibrous materials to reduce adhesion. However, as the following literature review shows, the developed products have certain limits, and their use for medical applications is still restricted.

Tang et al. have fabricated an antiadhesive material based on natural biopolymers agarose and collagen. The antiadhesive sheets were crosslinked with glutaraldehyde to support the mechanical behaviour. According to presented results, the materials show antiadhesive behaviour both *in vitro* (fibroblasts and adipose-derived adult stem) and *in vivo* (rabbit animal model) [8]. Although glutaraldehyde is widely used as a crosslinking agent, its toxicity and adverse effect on human health have been reported [9,10].

Antiadhesive materials can also be used for wound healing. By limiting the formation of adhesion between the wound and the patch, secondary tissue damage can be prevented when changing the dressing; an example of such material can be prepared via combination of alginates with gelatine [11]. However, the drawbacks of alginates include inappropriateness for dry wounds and poor dimensional properties leading to limited storage time [12]. In a study by Zhao et al., preparation of a material comprising antifibrotic mitomycin-C (MMC) has been described. The material structure was formed using so-called micro-sol electrospinning, which allows the preparation of core–shell nanofibers. The resulting structure led to a reduction in tendon adhesion, and the potential of using core–shell nanofibers with the active substance for the treatment of tendon injuries was shown [13]. The difficult controllability of MMC release and its potential adverse effects on human organisms pose as further limitations. Another studies have used nondegradable polymers such as polytetrafluoroethylene [14] or polyvinylidenfluorid [15]. Although these materials were shown to be antiadhesive, their application is significantly limited due to their non-biodegradable nature. According to the literature review, the introduced fibrous materials were mostly fabricated via laboratory-scale needle electrospinning. Commercially available products are not yet able to reliably prevent peritoneal adhesions [16,17].

The literature review reveals the difficulty of antiadhesive functionalization while maintaining the biocompatibility of the product. The main inspiration for this work was the superhydrophobic lotus leaf surface, which was simulated by the combination of needleless electrospinning and electrospraying. The developed scaffold is based on biocompatible and biodegradable poly-ε-caprolactone (PCL). The hierarchical structure is created by PCL nanofibers (NF) and PCL nanodroplets (ND), this combination creates the pure material, further denoted as NF + ND. The nanofibrous layer imitates the epidermis of the lotus leaf while nanodroplets mimick the papillae. The fabrication of scaffolds via the combination of electrospinning and electrospraying was already reported in the literature. For instance, Zhang et al. used the electrospun PCL/methyl silicone fibrous layers and PCL electrosprayed microspheres to fabricate a hierarchically structured surface for oil–water separation techniques, self-cleaning surfaces, or other applications [18]. Yoon et al. fabricated the PCL fibers and droplets in a one-step electrospinning process, which led to a superhydrophobic surface [19]. However, the scaffolds were not designed for primary use in medicine. Moreover, these attempts were based on low productive needle electrospinning with moderate homogeneity and repeatability. On the contrary, in this study, the highly productive needleless Nanospider™ was used. The Nanospider™ electrospinning device enables large-scale production, which supports the future introduction of the product to the market.

The superhydrophobic behavior of NF + ND was enhanced and supported since the papillae of the natural lotus leaf are also covered with epicuticular waxes. Thus, the surface of the antiadhesive side with electrosprayed ND was further modified by cold surface plasma treatment (PT) via chemical vapor deposition with hexamethyldisiloxane (HMDSO). The plasma treatment offers a low-cost process without altering the bulk material properties and is intensively used in biomedical research [20]. The advantage of HMDSO treatment is the biocompatibility and large hydrophobicity together with commercial availability; the lower bacterial adhesion to its surface was shown in [21]. Moreover, the process was already used for scaffold fabrication, Costoya et al. applied the HMDSO plasma treatment to PCL/cyclodextrin electrospun fibers for controlled drug delivery; the drug release rate was decreased due to an HMDSO hydrophobic barrier. The contact angle of the electrospun mat was increased to 130° [22]. Stloukal et al. treated other polyesters, namely polylactide acid and polyester urethane films with HMDSO and the decrease in chemotherapeutic drug release was directly proportional to the plasma treatment duration due to the growth of the HMDSO layer [23]. To our best knowledge,

we are the first group to introduce the plasma treatment of electrosprayed nanodroplets.

Herein, three layers with different time exposure to PT treatment (one, two, and three minutes) were fabricated; the different layers are denoted as NF + ND + PT_1min, NF + ND + PT_2min and NF + ND + PT_3min respectively. The hydrophobicity of the layers was increased with the increased time exposure. The cytocompatibility was proven during the *in vitro* testing with NIH/3T3 mouse fibroblasts. The absorption of water and simulated anastomotic leakage was measured. Moreover, the properties of the treated layers were observed during a six months period via FTIR spectroscopy and contact angle measurement to verify the stability of the treatment. The layers were tested *ex vivo* with the native intestinal tissue to prove the layers' antiadhesive behaviour. This approach helps to predict the material properties and reduce the number of tested animals during further *in vivo* studies.

2. Materials and methods

2.1. Materials

Solutions of 16% and 3% w/w PCL (M_W 45 000 g/mol, Sigma Aldrich, USA) were prepared by dissolving in chloroform/acetic acid/ethanol 8/1/1 (v/v/v) (Penta Chemicals, CZE). The solutions were stirred for 24 h until complete dissolution. The viscosity of the solutions was carried out by HAAKE™ RotoVisco™ 1 rheometer (Thermo Fisher Scientific, USA). The polymer solution (300 μl) was measured with constant revolution 1000 s^{-1} and speed 400 s^{-1}.

2.2. Electrospinning and electrospraying

First, a thin nanofibrous layer of average specific weight 7 g/m^2 was fabricated via needleless electrospinning device Nanospider™ 1WS500U (Elmarco, CZE) with controlled conditions by climatic system NS AC150 (Elmarco, CZE), the scheme of the Nanospider™ device is displayed on Fig. 1 - A. The fibrous layer was deposited on the polypropylene spunbond substrate and left to dry for 60 min. Subsequently, the nanodroplets were electrosprayed on the fibrous surface. The parameters of both processes are listed in Table 1.

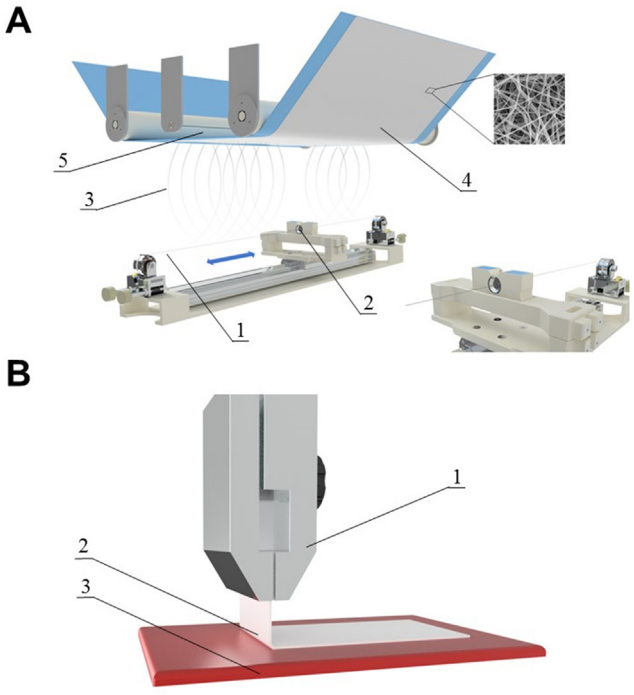

Fig. 1. Scheme of the needleless Nanospider electrospinning device: 1 – the positive electrode in the form of steel wire, 2 - steel orifice with a polymer solution reservoir, 3 – fiber/droplet formation and evaporation of the solvent, 4 - nanofibrous layer collected on a supporting textile material, 5 - steel wire serves as the negative electrode (A). Scheme of the 90° peel test. (B) Scheme of peel test 90°: 1 – load cell with a strain gauge, 2 – fibrous material, 3 – tissue model (pig's small intestinal tissue) placed on a table (B).

2.3. Plasma surface treatment

The surface plasma treatment (PT) was performed with hydrophobic hexamethyldisiloxane (HMDSO) by RF Frequency Plasma Assisted Chemical Vapor Deposition method in a vacuum chamber at low temperature with respect to the low melting point of PCL (around 60° C). The process was going under parameters (listed in Table 2), which were kept constant during the process.

2.4. Morphology, specific weight, and chemical structure of the layers

The morphology of fabricated layers was assessed by scanning electron microscopy (SEM), using a TESCAN VEGA 3 (SB Easy Probe, CZE). Firstly, samples were coated with a 7 nm layer of gold by QUORUM Q50ES (Quorum Technologies, GB). The NF and ND diameters (n = 500) were measured using IMAGE J (NIH Image, USA). The **specific weight** of the layers was calculated via the weighting of samples of dimensions of 20 × 20 mm (n = 6). **The chemical composition** was analysed via infrared spectroscopy ATR-FTIR method by Nicolet iZ10 (Thermo Fisher, USA). **The nanostructure** was observed with atomic force microscopy by Nanowizard3 AFM (JPK Instruments, Germany). The samples have been studied by point by point nanoindentation QI mode measurement with use of HQ:NSC19/Al BS cantilever with stiffness 0.5 N/m.

2.5. Contact angle measurement

The surface wettability was measured via the contact angle on both sides of the layers by the sessile drop method using the See System 6.2 (Advex Instruments, CZE) with a CCD camera. Samples with dimensions of 10 × 80 mm were fixed to microscopic slide and a droplet of distilled water (dH_2O) of volume 3.5 μl was applied on the surface of the sample and captured by the camera.

2.6. Absorption

The absorption of materials was evaluated by uptake of dH_2O and simulated intestine liquid. The methodology of absorption assessment was based on [24]. The simulated intestine liquid was prepared according to a procedure of Czech pharmacopeia. Following ingredients were mixed and appended up to 1000 ml with dH_2O and pH 6.8; 6.8 g monopotassium phosphate (KH_2PO_4, Lachema, CZE), in 250 ml of dH_2O, 77 ml potassium hydroxide 0.2 mol/l (NaOH, Penta Chemicals, CZE) 10 g pancreatin (CTI Chemicals, J). Samples with dimensions of 20 × 20 mm (n = 5) were placed into tubes with 50 ml of liquid and left 24 h at room temperature. Absorption (A) of the sample was calculated via the following formula.

$$A[\%] = \frac{m_B - m_A}{m_A} \cdot 100 \quad (1)$$

where m_A is a weight of the sample before testing, m_B is a weight of the sample after 24 h of soaking.

2.7. In vitro testing

Samples were firstly sterilized by ethylene oxide (Anprolene, USA) for 12 h at room temperature and aerated for at least one week to avoid possible residues in the layers.

Table 1
Process parameters of electrospinning and electrospraying via Nanospider™.

	Electrospinning		Electrospraying	
Concentration of PCL [%] w/w	16		3	
Viscosity [mPa·s]	278.7 ± 16.8		5.9 ± 0.9	
Distance between the electrodes [mm]	175		175	
High voltage [kV]	Electrode 1	Electrode 2	Electrode 1	Electrode 2
	−10	40	−5	35
Rewinding speed [mm/min]	80		5	
Cartridge movement speed [mm/s]	500		500	
Temperature [°C]	22		22	
Relative humidity [%]	50		50	

Table 2
Process parameters of surface plasma treatment (PT).

Vacuum pressure [Pa]	30
Frequence of RF generator [MHz]	13,5
Voltage [V]	340
Gas flow argon Ar [sccm]	10
Gas flow nitrogen N_2 [sccm]	7
Time [min]	1;2;3

Cytotoxicity was evaluated by the MTT assay after incubating 3 T3 fibroblasts with extracts of materials in full DMEM media (10 mg/ml of DMEM, extracted overnight at 37 °C, 100 rpm) for 24 h. The limit for cytotoxicity was 70% viability of control cells, called negative control (NC), according to the Czech norm ČSN EN ISO 10993–5 "Biological evaluation of medical devices - Part 5: In vitro cytotoxicity tests". The positive control (PC) stands for the incubated cells with the addition of 0,1% (v/v) Triton-X in media, which acts as a cytotoxic agent. The negative control (NC) means the cells incubated in pure DMEM.

Samples were seeded with 3 T3 fibroblasts (ATCC, USA) at a concentration of $7 \cdot 10^3$ cells/well. **The metabolic activity** of the cells was evaluated after 4, 7, and 14 days of cultivation by MTT assay and the cells were also visualized via fluorescence microscopy and SEM. During the MTT test, the samples were incubated with a solution of 250 µl MTT together with 750 µl of the complete media for 4 h at 37 °C, 5% CO_2; formazan crystals were dissolved in acidified isopropanol. The absorbance of the final solutions was measured at 570 and 690 nm (n = 5). For fluorescence analyses, phalloidin-FITC and DAPI were added to the samples to visualize cells. Cells were captured by fluorescence microscope Nikon Eclipse-Ti-E (Nikon Imagining, CZE), and the number of cells was quantified by MATLAB software. The details regarding the used methodology of *in vitro* testing were previously described in [25].

2.8. Mechanical testing of adhesive behavior ex vivo

The method was based on testing the adhesive behaviour of the materials to the native tissue with peel test 90° as shown in [26,27]. The adhesion was tested to the pig's small intestinal tissue. The experiment was carried out via LabTest 4.050 machine (LaborTech, CZE) and LabTest 3.2.1.2138 (LaborTech, CZE) software, which also provides an analytical and graphical evaluation of the results. A load cell strain gauge with a maximum load capacity of 5 N and a pin jaw for sample clamping was used to clamp the sample (see Fig. 1 – B). The sample size was (50 × 150) mm. The measurement was repeated five times for every tested material.

2.9. Statistics

The results were represented as mean ± standard deviation (SD). The statistical analysis was done via GraphPad Prism 7 (GraphPad Software, USA) via parametric 2-way ANOVA with Bonferroni multiple comparison test for normally distributed data or nonparametric Kruskal-Wallis test for data that did not correspond to the normal distribution. Values of $p \leq 0.05$ were considered significant.

3. Results

3.1. Morphology

The morphology of prepared layers, together with graphs of NF or ND diameters with outliers and a schematic indication of the lotus leaf inspiration and the resulting structure, is shown in Fig. 2. The nanofibrous planar layer was fabricated via needleless electrospinning. From a macroscopic point of view, the layer was uniform, without visible defects. According to SEM images (Fig. 2 - A), NFs were unoriented, disorganized, and defect-less with thin diameters of (180 ± 177) nm. The high SD is caused by the occurrence of ultrafine fibers together with larger ones. Nanodroplets were created by applying needless electrospraying of 3% PCL on the surface of the fibrous layer. These NDs imitate the papillae on the lotus leaf, as shown in Fig. 2 – C. The forementioned conditions had been successfully optimized based on several experiments of needle- and needless electrospraying. The change of surface morphology was also visible from a macroscopic point of view. Drops on the surface were unorganized with a diameter (198 ± 98) nm.

The plasma surface treatment created a thin layer on the surface of the nanodroplets, which was primarily visible at the layer with the most prolonged exposition (NF + ND + PT_3 min) with lower magnification (Fig. 2 - A). The PT modification mimics the hydrophobic epicuticular waxes of the natural lotus plant. Plasma modification was homogenous in the NF + ND + PT_1min and NF + ND + PT_2min (Fig. 2 - C and Fig. 2 - D). The diameter of the treated ND was increased in correlation with growing time exposure to (592 ± 164) nm, resp. (631 ± 225) nm. The NF + ND + PT_3min contained irregularly occurring places, which resembled a film structure and the highest droplet diameter (780 ± 310) nm. The plasma treatment was also noticeable from a macroscopic point of view by the change of colour of the layers (data not shown).

3.2. Wettability, surface and chemical structure

Wettability was measured via contact angle measurement; results are shown in Fig. 3 - A. The contact angle of the pure NF was (99 ± 3)°. The process of electrospraying did not significantly influence the wettability of the surface since the contact angle on the side of the material with ND was (103 ± 5)°. The contact angle of plasma modified layers confirmed the assumption about the hydrophobicity of HMDSO. Wettability was successfully decreased by plasma modification in comparison with not treated PCL layer. After 1 and 2 min modification, hydrophobicity of the surface

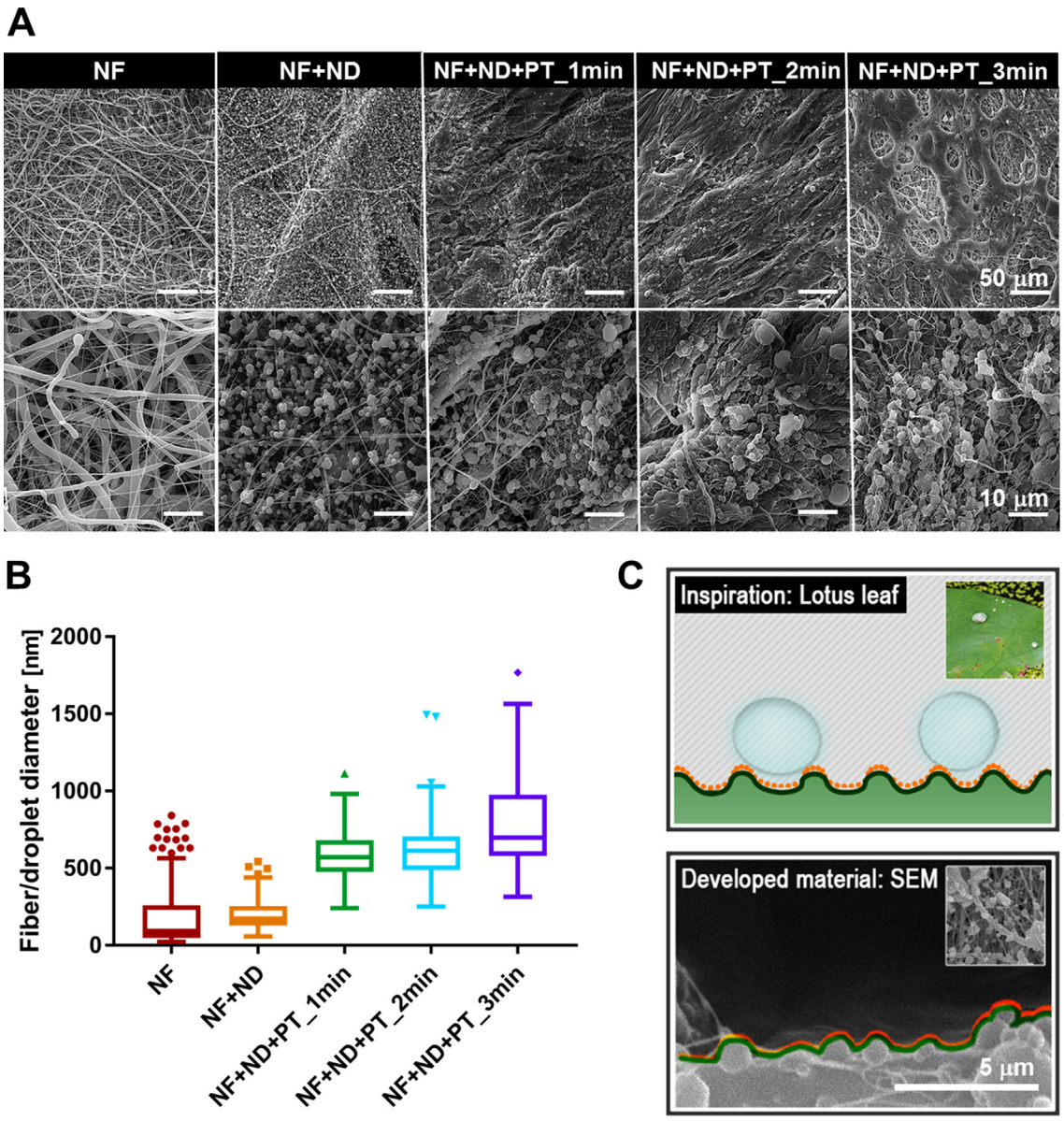

Fig. 2. SEM images of fabricated materials, scale bars 10 and 50 µm (A), graph with NF and ND diameters (n = 500) (B) and schematic illustration of the lotus leaf structure together with the side view of the produced material, scale bars 5 µm (C).

increased to (112 ± 7)° and (115 ± 6)°. The most hydrophobic, therefore with the least wettability material was gained by 3 min plasma treatment, the contact angle of the surface was (125 ± 3)°.

The change to surface properties resulting from the plasma modification with HMDSO is attributed to chemical bonds between C-O, Si-O, Si-C, and Si-H, shown in the spectra from FTIR analysis (Fig. 3 - B). In the significant Si peak, the intensity of the spectrum corresponds with the duration of the modification. Spectra of the NF and ND layer were identical, which corresponds with their chemical composition.

The presence of surface water and surface adhesion was further investigated by AFM. The surface topology is presented in Fig. 4, where we present (from the left) the surface topology, 3D image of the topology and last not least the adhesion map. From the measured force AFM curves we estimated the adhesion force via the software provided by the AFM manufacturer. For relative comparison between the measurement brand new cantilever was used and we measure from the less adhesive sample to the more adhesive sample. The humidity in the room was 54%. The adhesive forces were around (9.5 ± 1.7) nN for the 0 min treated plasma and (0.8 ± 0.5) nN for the 3 min plasma treated samples. In here we can see difference in one order of magnitude in the adhesion forces, which are mostly caused by presence of water on the sample and the sample adhesivity. The errors of the measurement are relatively high, this was caused by nature of the sample, since the nanofibers tend to swing when compressed by the cantilever, that also creates the blur artefact on some nanofibers at the topographical images. The measurement was also complicated by high aspect ratio of the samples which are on the borderline of AFM piezo capabilities. Nevertheless, the obtained results provide great insight in the nano-mechanical properties of the sample.

3.3. FTIR structure and time stability of plasma treatment

After the plasma treatment, the presence of HMDSO was evaluated for six months directly by chemical composition and indirectly by measuring the contact angle. Intervals were chosen based on the expected period of material's required functionality

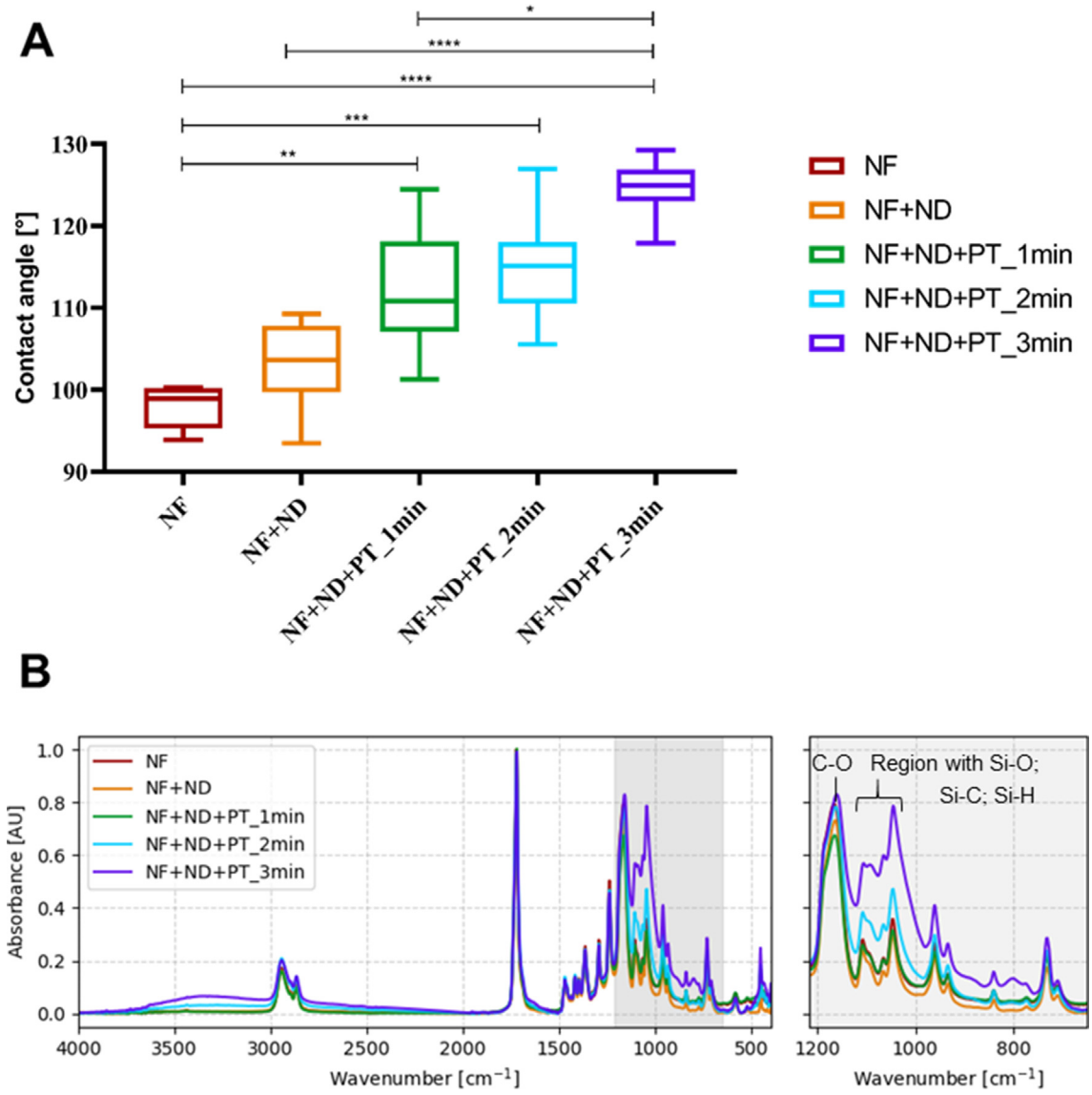

Fig. 3. Contact angles of tested materials, n = 10, (ANOVA, Kruskal-Wallis); * p < 0,0332, ** p < 0,0021, **** p < 0,0001 (A); the FTIR spectra with the characteristic peak for PCL and HMDSO (labelled), the presence of siloxane group increases with the growing time exposure (B).

during tissue healing. The critical period is 14 days after the surgery. The primary *in vivo* experiments were held for 21 days [17], also based on the potential storage time of the material prior to its application.

Results of the contact angle measurement are shown in Fig. 5 - A. There were no significant changes in wettability within NF layers during the measured period. However, measurable increase in the contact angles of materials with PT was detected. The contact angle of NF + ND + PT_3min was (131 ± 4°) in comparison with day 1 (125 ± 3)°. Obtained FTIR spectra also support this observation. The bounds created by the plasma modification were still present after six months, even in higher intensities. The growing trend was found in every material, and Fig. 5 - B reveals the NF + ND + PT_3min spectra as an example.

3.4. Uptake of distilled water and simulated intestine liquid

The behaviour of the fabricated scaffolds *in vivo* can also be predicted via the interaction with simulated body fluids. The results plotted in Fig. 6 show the absorption of distilled water (A_W [%]) and simulated intestine liquid (A_S [%]). The statistically most significant difference was between plasma modified layers in comparison with the nanofibrous layer. The untreated NF exhibit the greatest uptake of both liquids (A_W = 414.0 ± 41.3%; A_S = 501.7 ± 7 5.0%). On the contrary, the plasma modified layers absorbed less liquid, which corresponds with the lower surface energy of the material. There was no significant difference between layers NF + ND + PT_1min and NF + ND + PT_2min; absorption of both materials was about 30%. Layer NF + ND + PT_3min had slightly higher absorption (A_W = 79.4 ± 5.0%; A_S = 89.4 ± 12.4%).

Different behaviour of distilled water and the simulated intestine liquid is most likely attributed to different surface tension of these liquids.

3.5. In vitro testing

Viability and proliferation assessments were evaluated based on the measurement of metabolic activity of fibroblasts. Results of cytotoxicity assessment are shown in Fig. 7. Viability of fibroblasts after incubation with material's extracts did not drop below

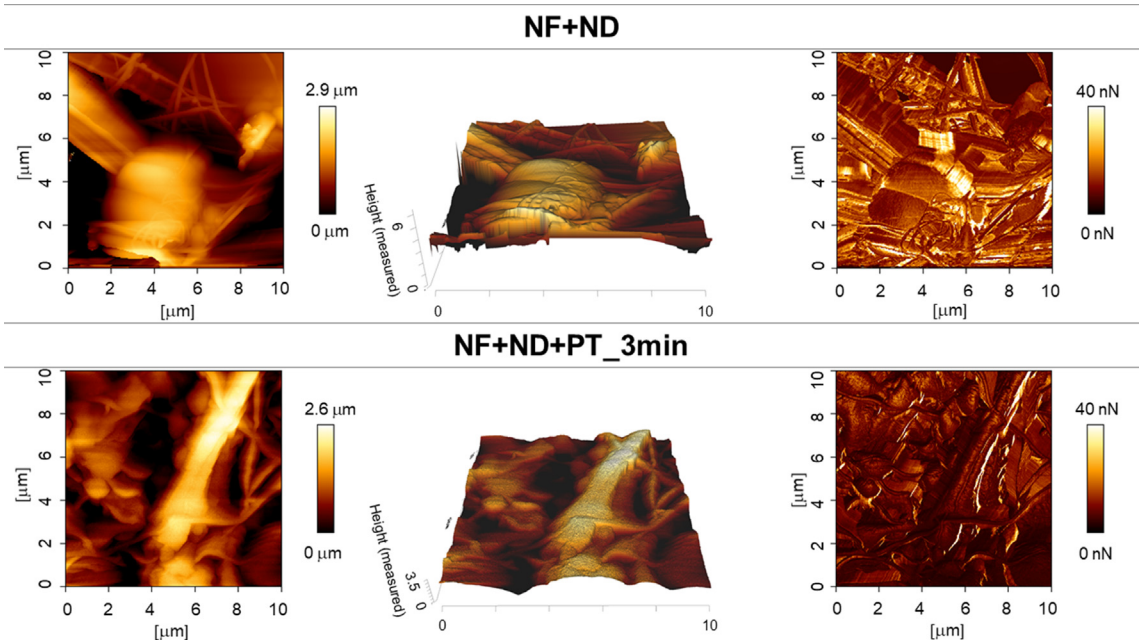

Fig. 4. Left to right nanotopology of the sample; 3D image of topology; adhesion map of the sample.

the 70% toxic line/limit. Therefore, the plasma-treated materials are considered non-cytotoxic.

Fig. 7 - C shows the results of the proliferation assessment. There were no significant differences between tested materials on day 4 (first testing day). Fibroblast proliferation significantly rose on day 7, especially with the NF + ND + PT_1min layer. There was an increase of proliferation on day 14 of all tested materials, excluding the NF + ND + PT_1min layer. The viability of cells seeded on this material slightly decreased, probably due to the achievement of full cell confluence. After 14 days of incubation, there was no significant difference between the tested layers.

Besides that, the proliferation assessment was based on microscopy analysis and cell quantification (Fig. 7 - B). According to fluorescence images in Fig. 8, cells spread gradually across the samples of all tested layers during 14 days of incubation. The most significant proliferation was on the NF + ND + PT_1min and NF + ND + PT_3min sample on day 14. In the end, samples with plasma modification carried a continuous cell layer, the number of cells was estimated as (6155 ± 1186) cells/1mm^2 for NF + ND + PT_1 min, (5023 ± 1935) cells/1mm^2 for NF + ND + PT_2min and (4541 ± 1222) cells/1mm^2 cell number for NF + ND + PT_3min. The number of cells for NF and NF + ND was comparable, approximately 4200 cells/1mm^2.

3.6. Ex vivo antiadhesive behavior

The initial testing of adhesive properties of the developed materials was performed via mechanical tensile test (peel test 90°). The small intestine was chosen as a tissue model based on preliminary *in vivo* testing on piglets with pure PCL nanofibrous mats, see [17]. Fig. 9 - A shows the maximum forces of the tested materials required to detach them from the intestinal surface; the obtained results confirm the potential application of the developed structure for tissue adhesion prevention (Fig. 9 - B). The greatest adhesion was demonstrated by the fibrous material with the maximum force (352.5 ± 50.0) mN. The adhesion of the samples with spraying, NF + ND, did not significantly differ with the maximum force of (337.5 ± 94.7) mN. Materials with plasma treatment are less adhesive compared to unmodified layers: the NF + ND + PT_1min, resp. NF + ND + PT_2min show the adhesive force (292.5 ± 22.2) mN, resp. (222.5 ± 31.6) mN. The most statistically significant difference occurred between the NF and NF + ND + PT_3min, where the maximum force required for detaching the material from intestinal tissue was (203.0 ± 20.0) mN (see Fig. 9 - B).

4. Discussion

This study introduces a novel nanofibrous material with an antiadhesive surface for preventing severe postoperative adhesions. There are many developed materials to solve peritoneal adhesions [28–30]. However, there are currently no commercially available products commonly used in clinical practice during abdominal surgeries since they have shown limited advantages. Therefore, there is an urgent need to develop a material that prevents life-threatening postoperative adhesions [16,17].

Our material consists of biodegradable poly-ε-caprolactone. The choice of the polymer was based mainly on the excellent biocompatibility of PCL and the preliminary animal *in vivo* results of our previous study by Rosendorf et al. [17]. Our previous research has also shown that pure PCL nanofibers exhibit adhesive behaviour to intestinal tissue. In this work, the PCL-based material was modified with additional, biomimicking antiadhesive layer. The morphology of the antiadhesive layer was inspired by the surface morphology of the lotus leaf, which is well known for its superhydrophobic behavior due to the hierarchical structure of the epidermis, papillae, and epicuticular waxes described in [4,31]. The material was fabricated via the combination of needleless electrospinning and electrospraying. Electrospinning is a well-known technology for scaffold fabrication [32] and was already used in combination with electrospraying [18,19]. In this study, the needleless NanospiderTM was used with advantages like large-scale production, well-controlled process parameters, and easy repeatability.

The randomly oriented fibrous morphology corresponds with [33] and the median fiber diameter (180 ± 177) nm is consistent with the study Horakova et al., where the same solvent system and concentration of PCL were used [34]. The electrosprayed microspheres were applied to the fibrous PCL materials to mimic

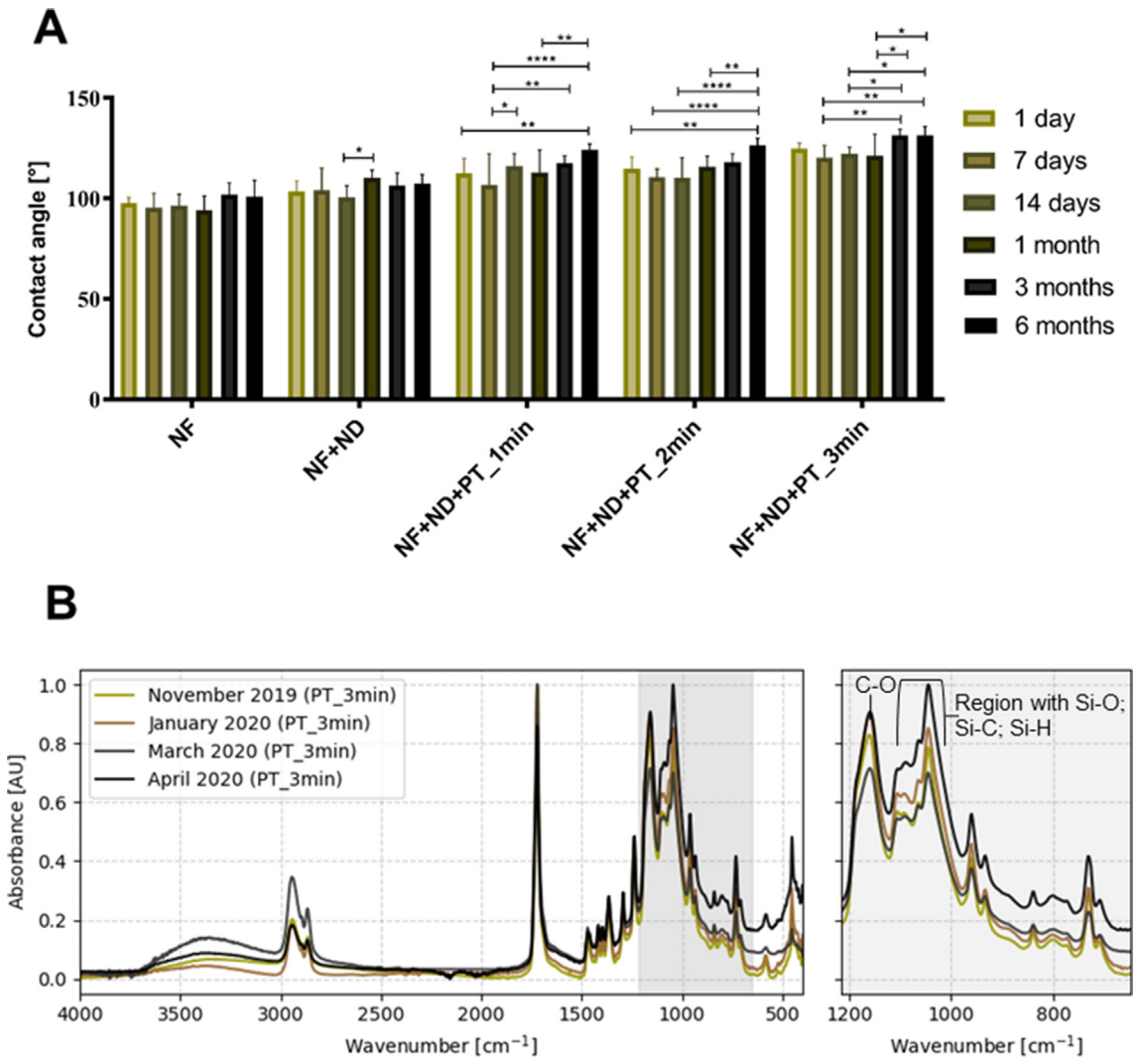

Fig. 5. Measured contact angle of tested materials in period of six months (n = 10); * p < 0,0332, ** p < 0,0021, *** p < 0,0002, **** p < 0,0001 (ANOVA, Bonferroni) (A); FTIR structure revealing the presence of characteristic siloxane group (labelled) during 6 months observation (B).

the hierarchical lotus leaf structure, shown in Fig. 2 – C. The presence of ND did not lead to sufficient change of surface energy. Zhang et al. reported increased contact angle (146.0 ± 2.8)° from (120.0 ± 1.3)° just by the combination of electrospinning and electrospraying of PCL. However, in their study, the substrate consists of PCL and methyl silicone oil fabricated from the different solvent system (chloroform/N-dimethylformamide 4:1 v/v). The size of the droplets (6.711 ± 1.492) μm fabricated by needle electrospraying of 4% PCL solutions was larger than the diameters obtained in this work (198 ± 98) nm [18].

The layer combining electrospinning and electrospraying was further modified with plasma treatment by HMDSO. This modification was chosen because of the biocompatibility and the hydrophobic effect of HMDSO, mentioned in [35,36]. The advantages of plasma modification include low cost of the process and preservation of bulk properties of the nanofiber scaffold; this statement is confirmed by study Martins et al. [20]. After plasma modification, a thin film of HMDSO covered the surface of the electrosprayed nanospheres and is evident from the SEM images (Fig. 2 – A).

The effects of the plasma treatment were further evaluated by measuring the contact angle with distilled water. Compared to the untreated layer (99 ± 3)°, the hydrophobicity of the surface increased, and the contact angle (125 ± 3)° was measured for the layer with a 3-minute modification. The chemical structure of the treated materials was analyzed by FTIR, which confirmed the presence of Si- bonds, which are typical for siloxane treatments [36]. The temporal stability of the modified layer was observed for six months without any significant changes. Similarly, the time stability of the wettability of siloxane plasma-treated polycarbonate layers was also observed by Hegemann et al., who did not notice a significant difference in the contact angle during 12 months [37]. The treatment did not affect the fibrous PCL side of the material, which was not under exposure. The additional contact angle measurement confirmed no measurable changes in wettability. Hence, the adhesion properties of the untreated side were not influenced. The atomic force microscopy confirmed the less adhesive properties of the plasma treated samples.

The plasma-modified materials show minimal absorption of distilled water and simulated intestinal fluid compared to the pure nanofibrous layer and the fibrous layer covered with electrosprayed nanospheres; no statistically significant differences between samples with different treatment times were notified. This correlates well with the observation of treated materials' reduced surface energy, which lowers the ability to absorb. Absorption tests showed different behaviour towards distilled water and simulated intestinal fluid, probably due to different sur-

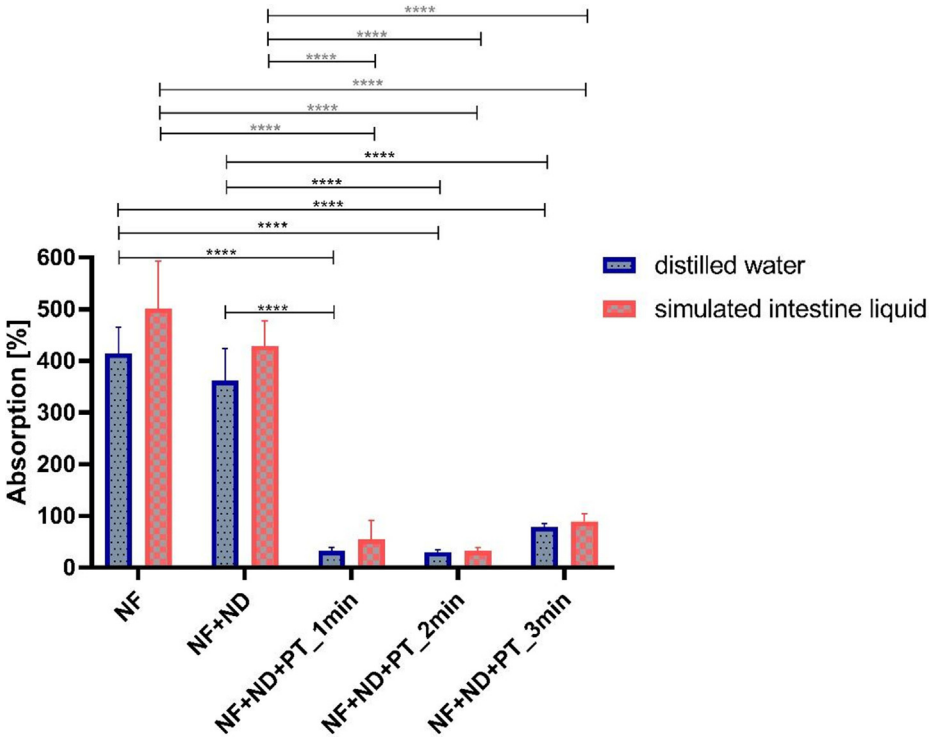

Fig. 6. Uptake of distilled water and simulated intestine liquid, n = 5, (ANOVA, Bonferroni); *** p < 0,0002, **** p < 0,0001.

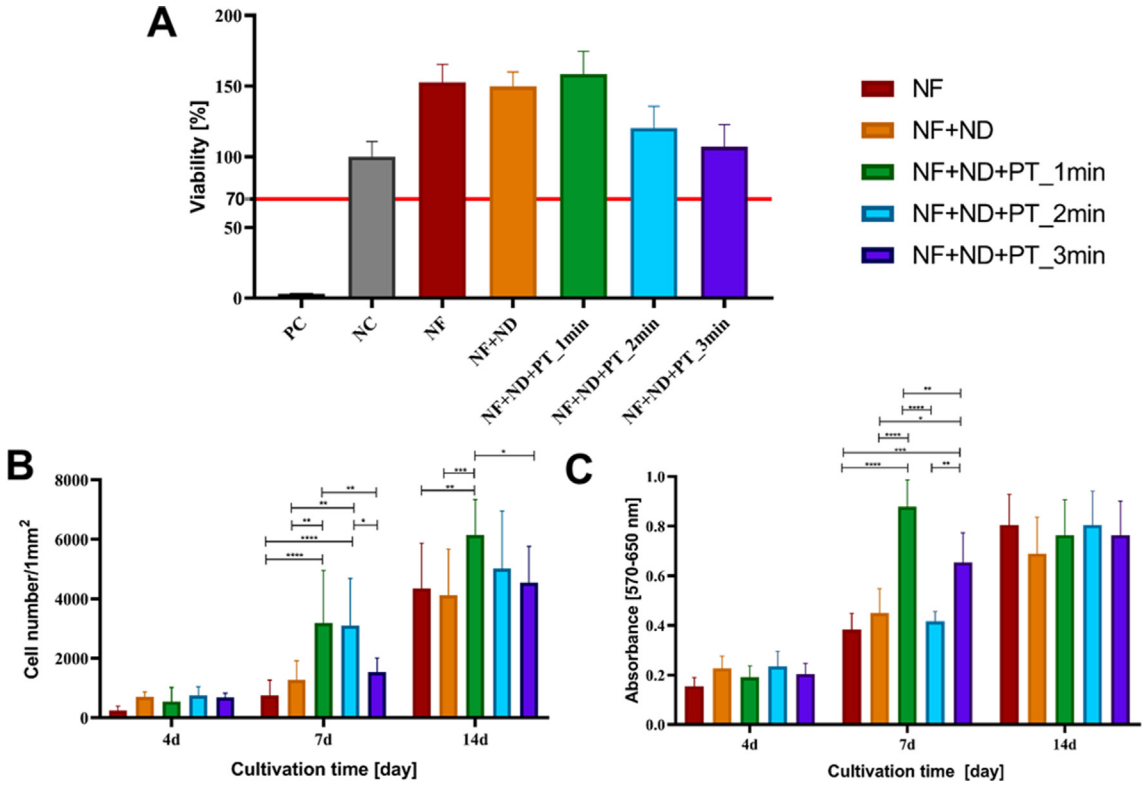

Fig. 7. Graf of cytocompatibility of all tested materials, PC and NC stands for positive, resp. negative controls (A). Results of number of calculated cells on the surfaces per 1 mm^2 (B) and metabolic MTT assessment (C) after 4, 7 and 14 days of cultivation with 3 T3 mouse fibroblasts; n = 8, (ANOVA, Bonferroni); * p < 0,0332, ** p < 0,0021, *** p < 0,0002, **** p < 0,0001.

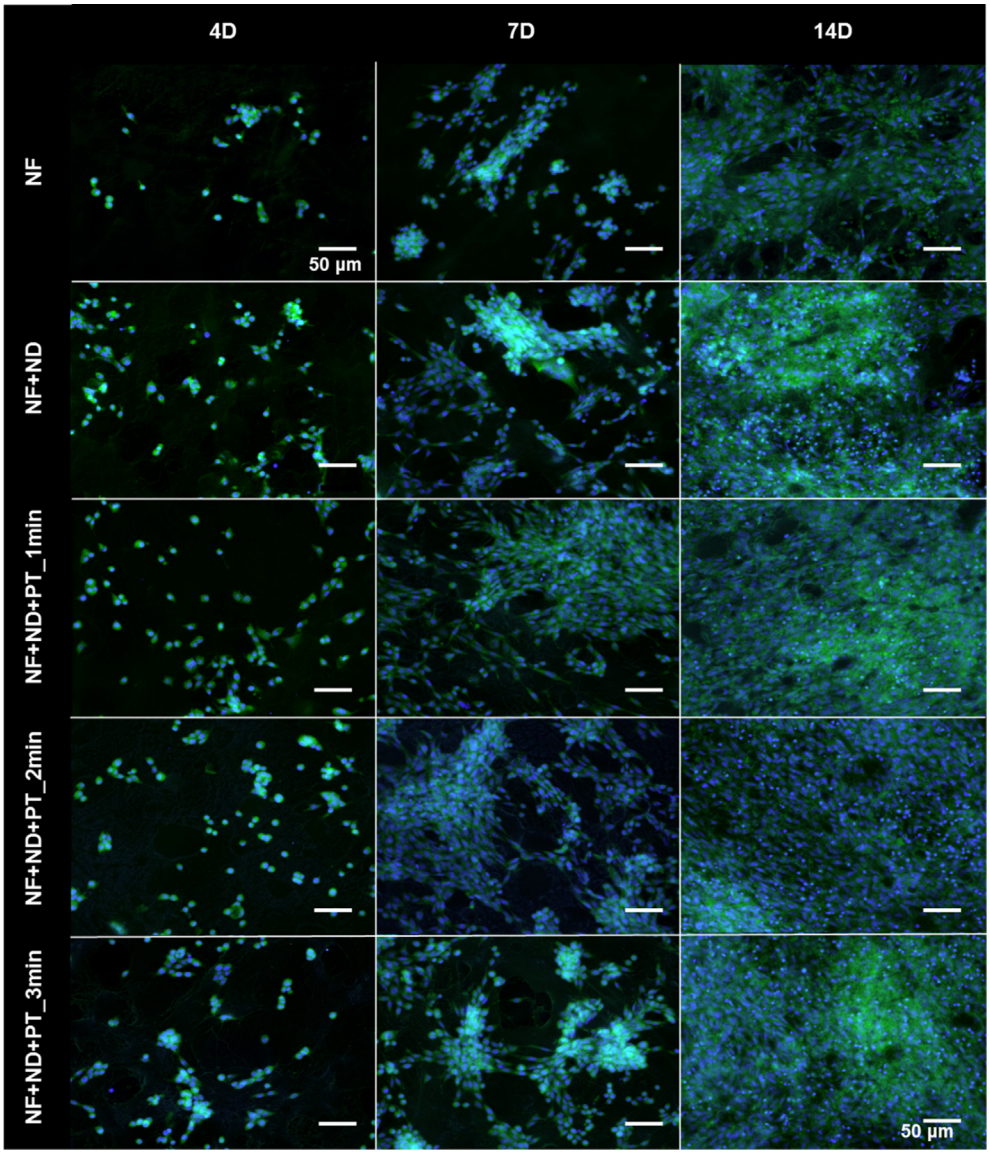

Fig. 8. Fluorescence microscopy images of fibroblasts after 4, 7, and 14 days of cultivation; scale bar 50 µm.

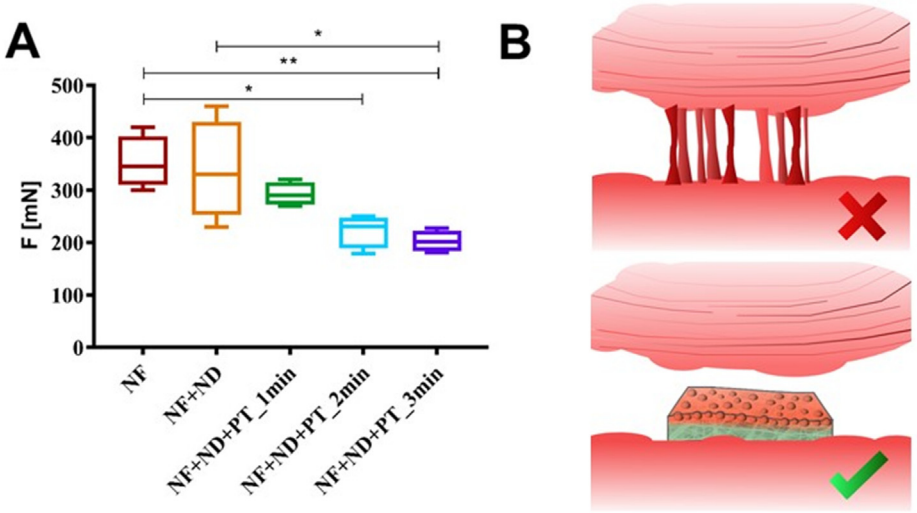

Fig. 9. Results of peel test 90° with all fabricated materials, hydrophobic treatment led to decreased adhesion to intestinal tissue (A). Material serves as a potential barrier prevention of the undesired tissue adhesions (B).

face tensions. The surface tension of distilled water is 73 mN/m; for intestinal fluid, it is around 32 mN/m [38].

The non-toxicity of HMDSO treatment and its use for medicine was described in Siow et al. or Bacakova et al. [6,36]; these statements correlate with our observation. The cytocompatibility of developed materials was confirmed by *in vitro* tests. The cell adhesion and proliferation were also tested *in vitro*; the metabolic MTT test results after 14 days cultivation of mouse fibroblasts with the materials did not distinguish statistically significant changes throughout the groups. The results from fluorescence microscopy differed slightly. The layer with a 1-minute treatment showed a significant increase in cell numbers after 14 days compared to other materials. All tested materials were sterilized with low-temperature ethylene oxide prior to cell seeding; the possible effect of sterilization on the treatment of PCL nanofibers was already investigated in our previous study by Horakova et al. [34].

The *ex vivo* adhesion testing of the fabricated materials to intestinal tissue was shown in our study. Similar approaches are known for estimating skin adhesion described by Wokovich et al. and other studies [26,27]. However, the available literature sources did not reveal any mechanical testing of nanofibers with intestinal tissue. This experiment was chosen to predict the behaviour of the materials in contact with native tissue in the abdominal cavity. Since *in vivo* testing with animal models is indispensable but very costly and time-consuming, this approach allows to reduce the number of tested animals. The results of the initial mechanical tests of adhesions to the pig intestine confirmed our hypotheses. The magnitude of the force required to peel the material from the intestinal tissue decreased with hydrophobic plasma treatment. In contrast, the PCL nanofiber layer showed the highest adhesion. The pure PCL layers were shown to be adhesive also *in vivo* [17].

The obtained results revealed the most appropriate time of the plasma surface treatment to be a two minute exposure (material NF + ND + PT_2min). The one-minute modification was not sufficiently homogeneous, and the hydrophobic effect was minimal compared to the materials treated for two and three minutes. The SEM images (see Fig. 2) detected major morphology change in the NF + ND + PT_3min material, where the treatment led to the creation of the non-homogenous HMDSO film. Such modification is undesirable; the film deposition could reduce the porosity of the material, which has been confirmed *in vivo* to be crucial for the cell migration and overall healing of the tissue. The material will be further tested *in vivo* (animal pig model) to testify the antiadhesive behaviour of the introduced material to the living tissue in a dynamical body environment.

5. Conclusion

We successfully developed a planar nanofibrous layer with different wettability on each side. The hydrophobic side consists of a structured, lotus leaf-like surface. The surface is comprised of nanofibers, electrosprayed droplets and a hydrophobic layer created by plasma surface treatment. Conditions of needleless electrospraying were successfully optimized within this work via Nanospider™, which allows for industrial-scale production. The plasma modification effectively increased the contact angle of the surface up to (125 ± 5)°; *in vitro* testing confirmed the non-cytotoxicity of produced materials. The manufactured material with both antiadhesive and adhesive sides has a great potential to effectively prevent postoperative adhesions in tendon, peritoneal area, dura mater, or pelvis. The fabricated materials will be further tested *in vivo* with a piglet animal model; however, *ex vivo* testing with native tissue confirmed the desirable lower adhesion of the developed materials and fulfilled our hypotheses.

Declaration of Competing Interest

The authors declare that they have no known competing financial interests or personal relationships that could have appeared to influence the work reported in this paper.

Acknowledgement

The research was supported by the project Czech Health Research Council (MZ ČR AZV) NU20J-08-00009 Prevention of intestinal anastomotic leakage and postoperative adhesions by using nanofibrous biodegradable materials. A. Fucikova would like to thank the UNCE/SCI/01.

References

[1] W. Wu, R. Cheng, J. das Neves, J. Tang, J. Xiao, Q. Ni, X. Liu, G. Pan, D. Li, W. Cui, B. Sarmento, Advances in biomaterials for preventing tissue adhesion, J. Controlled Release 261 (2017) 318–336.
[2] V. Mais, Peritoneal adhesions after laparoscopic gastrointestinal surgery, World J. Gastroenterol. WJG 20 (17) (2014) 4917, https://doi.org/10.3748/wjg.v20.i17.4917.
[3] M.A. Woodruff, D.W. Hutmacher, The return of a forgotten polymer—Polycaprolactone in the 21st century, Prog. Polym. Sci. 35 (2010) 1217–1256.
[4] E.J. Falde, S.T. Yohe, Y.L. Colson, M.W. Grinstaff, Superhydrophobic materials for biomedical applications, Biomaterials 104 (2016) 87–103.
[5] X. Wang, B. Ding, J. Yu, M. Wang, Engineering biomimetic superhydrophobic surfaces of electrospun nanomaterials, Nano Today 6 (5) (2011) 510–530.
[6] L. Bacakova, E. Filova, M. Parizek, T. Ruml, V. Svorcik, Modulation of cell adhesion, proliferation and differentiation on materials designed for body implants, Biotechnol. Adv. 29 (2011) 739–767.
[7] D.P. Dowling, I.S. Miller, M. Ardhaoui, W.M. Gallagher, Effect of Surface Wettability and Topography on the Adhesion of Osteosarcoma Cells on Plasma-modified Polystyrene, J. Biomater. Appl. 26 (3) (2011) 327–347, https://doi.org/10.1177/0885328210372148.
[8] S. Tang, W. Yang, X. Mao, Agarose/collagen composite scaffold as an anti-adhesive sheet, Biomed. Mater. Bristol Engl. 2 (3) (2007) S129–S134.
[9] T. Takigawa, Y. Endo, Effects of glutaraldehyde exposure on human health, J. Occup. Health 48 (2006) 75–87.
[10] H. Park, S. Baek, H. Kang, D. Lee, Biomaterials to Prevent Post-Operative Adhesion, Materials 13 (14) (2020) 3056.
[11] J. Sun, H. Tan, Alginate-Based Biomaterials for Regenerative Medicine Applications, Materials 6 (4) (2013) 1285–1309.
[12] R. Gheorghita Puscaselu, A. Lobiuc, M. Dimian, M. Covasa, From Food Industry to Biomedical Applications and Management of Metabolic Disorders, Polymers 12 (10) (2020) 2417, https://doi.org/10.3390/polym12102417.
[13] X. Zhao, S. Jiang, S. Liu, S. Chen, Z.Y. Lin, G. Pan, F. He, F. Li, C. Fan, W. Cui, Optimization of intrinsic and extrinsic tendon healing through controllable water-soluble mitomycin-C release from electrospun fibers by mediating adhesion-related gene expression, Biomaterials 61 (2015) 61–74.
[14] A. Lladó, E. Sologaistua, J. Guimerá, M. Marín, Expanded polytetrafluoroethylene membrane for the prevention of peridural fibrosis after spinal surgery: a clinical study, Eur. Spine J. Off. Publ. Eur. Spine Soc. Eur. Spinal Deform. Soc. Eur. Sect. Cerv. Spine Res. Soc. 8 (1999) 144–150.
[15] A. Klapstova et al., A PVDF electrospun antifibrotic composite for use as a glaucoma drainage implant, Mater. Sci. Eng. C Mater. Biol. Appl. 119 (2021) 111637.
[16] J.E. Ko, Y.-G. Ko, W.I. Kim, O.K. Kwon, O.H. Kwon, Nanofiber mats composed of a chitosan-poly(d, l-lactic-co-glycolic acid)-poly(ethylene oxide) blend as a postoperative anti-adhesion agent, J. Biomed. Mater. Res. B Appl. Biomater. 105 (2017) 1906–1915.
[17] J. Rosendorf et al., Experimental fortification of intestinal anastomoses with nanofibrous materials in a large animal model, Sci. Rep. 10 (2020) 1–12.
[18] G. Zhang, P. Wang, X. Zhang, C. Xiang, L. Li, Preparation of hierarchically structured PCL superhydrophobic membrane via alternate electrospinning/electrospraying techniques, J. Polym. Sci. Part B Polym. Phys. 57 (2019) 421–430.
[19] H. Yoon, J.H. Park, G.H. Kim, A Superhydrophobic Surface Fabricated by an Electrostatic Process, Macromol. Rapid Commun. 31 (2010) 1435–1439.
[20] A. Martins et al., Surface modification of electrospun polycaprolactone nanofiber meshes by plasma treatment to enhance biological performance, Small Weinh. Bergstr. Ger. 5 (2009) 1195–1206.
[21] R.A. Tupinambá, C.A. de A. Claro, C.A. Pereira, C.J.P. Nobrega, A.P.R.A. Claro, Bacterial adhesion on conventional and self-ligating metallic brackets after surface treatment with plasma-polymerized hexamethyldisiloxane, Dent. Press J. Orthod. 22 (2017) 77–85.
[22] A. Costoya et al., HMDSO-plasma coated electrospun fibers of poly (cyclodextrin)s for antifungal dressings, Int. J. Pharm. 513 (2016) 518–527.
[23] P. Stloukal et al., Effect of plasma treatment on the release kinetics of a chemotherapy drug from biodegradable polyester films and polyester urethane films, Int. J. Polym. Mater. Polym. Biomater. 67 (2018) 161–173.

[24] E.J. Choi, B. Son, T.S. Hwang, E.-H. Hwang, Increase of degradation and water uptake rate using electrospun star-shaped poly(d, l-lactide) nanofiber, J. Ind. Eng. Chem. 17 (2011) 691–695.
[25] J. Horakova et al., The effect of ethylene oxide sterilization on electrospun vascular grafts made from biodegradable polyesters, Mater. Sci. Eng. C Mater. Biol. Appl. 92 (2018) 132–142.
[26] A.M. Wokovich, S.A. Brown, F.J. McMaster, W.H. Doub, B. Cai, N. Sadrieh, M.L. Chen, S. Machado, M. Shen, L.F. Buhse, Evaluation of substrates for 90° peel adhesion—A collaborative study. I. Medical tapes, J. Biomed. Mater. Res. B Appl. Biomater. 87B (1) (2008) 105–113.
[27] M. Baumgartner et al., Resilient yet entirely degradable gelatin-based biogels for soft robots and electronics, Nat. Mater. 19 (2020) 1102–1109.
[28] H. Capella-Monsonís, S. Kearns, J. Kelly, D.I. Zeugolis, Battling adhesions: from understanding to prevention, BMC Biomed. Eng. 1 (2019) 5.
[29] G.M. Bürgisser, J. Buschmann, History and performance of implant materials applied as peritendinous antiadhesives, J. Biomed. Mater. Res. B Appl. Biomater. 103 (2015) 212–228.
[30] R.P.G. ten Broek, M.W.J. Stommel, C. Strik, C.J.H.M. van Laarhoven, F. Keus, H. van Goor, Benefits and harms of adhesion barriers for abdominal surgery: a systematic review and meta-analysis, The Lancet 383 (9911) (2014) 48–59.
[31] R. Hensel, C. Neinhuis, C. Werner, The springtail cuticle as a blueprint for omniphobic surfaces, Chem. Soc. Rev. 45 (2016) 323–341.
[32] Y. Ding et al., Electrospun Fibrous Architectures for Drug Delivery, Tissue Engineering and Cancer Therapy, Adv. Funct. Mater. 29 (2019) 1802852.
[33] R. Jirkovec, J. Erben, P. Sajdl, J. Chaloupek, J. Chvojka, The effect of material and process parameters on the surface energy of polycaprolactone fibre layers, Mater. Des. 205 (2021) 109748.
[34] J. Horakova, M. Klicova, J. Erben, A. Klapstova, V. Novotny, L. Behalek, J. Chvojka, Impact of Various Sterilization and Disinfection Techniques on Electrospun Poly-ε-caprolactone, ACS Omega 5 (15) (2020) 8885–8892.
[35] P. Dg, T. Si, A. Yg, Plasma treatment as an efficient tool for controlled drug release from polymeric materials: A review, J. Control. Release Off. J. Control. Release Soc. 266 (2017) 57–74.
[36] K.S. Siow, Low pressure plasma modifications for the generation of hydrophobic coatings for biomaterials applications, Plasma Process. Polym. 15 (2018) 1800059.
[37] D. Hegemann, H. Brunner, C. Oehr, Plasma treatment of polymers for surface and adhesion improvement, Nucl. Instrum. Methods Phys. Res. Sect. B Beam Interact. Mater. At. 208 (2003) 281–286.
[38] D.M. Mudie, G.L. Amidon, G.E. Amidon, Physiological Parameters for Oral Delivery and in Vitro Testing, Mol. Pharm. 7 (2010) 1388–1405.